IEEE Access
Multidisciplinary | Rapid Review | Open Access Journal

Received January 22, 2019, accepted February 4, 2019, date of publication February 26, 2019, date of current version March 20, 2019.

Digital Object Identifier 10.1109/ACCESS.2019.2901090

The Fast Measurement for the Relative Position of Flange-End Holes

LEI WANG[1,2], GANG LU[2], AND YING SUN[2]
[1]Tianjin Key Laboratory of Wireless Mobile Communications and Power Transmission, Tianjin Normal University, Tianjin 300387, China
[2]State Key Laboratory of Precision Measuring Technology and Instruments, Tianjin University, Tianjin 300072, China

Corresponding author: Lei Wang (wanglei2014@tju.edu.cn)

This work was supported in part by the Doctoral Foundation of Tianjin Normal University (52XB1906), and in part by the National Science and Technology Major Project of China under Grant 2016ZX04003001.

ABSTRACT For the flange end of the internal combustion engine crankshaft, the position of threaded holes and pinhole relative to the journal reference plane affects the dynamic balance and thermal efficiency of the engine, and therefore, this parameter measurement has a positive significance in the crankshaft manufacture. This paper proposes a system for quickly measuring the relative position of the flange-end holes, which uses a pneumatic linear variable differential transformer to form measuring benches for getting the position of the journal reference plane, and the high precision coordinates of the flange-end holes are obtained by multi-camera. The coordinates of the flange-end holes are merged into the global coordinate system of the journal reference plane, and the experimental result shows that the position uncertainty is better than 0.1 mm. This method has the advantage of convenient loading and unloading, fast measuring speed, and high accuracy and is easily implemented in the flexible manufacturing line for a full inspection of the semi-finished crankshaft.

INDEX TERMS Crankshaft, flange-end holes, pLVDT, multi-camera.

I. INTRODUCTION

Crankshaft is an important part of the internal combustion engine. It converses the reciprocating motion of the piston to the rotating motion, and endures the impulsive loading for power output. There are usually multiple threaded holes and one pin hole in the flange-end of the crankshaft. Threaded holes are used to fix the flywheel, and the fly-wheel has a powerful rotational inertia that can store the energy and inertia of the engine beyond the work stroke, so that the crankshaft can rotates at a constant speed. The pin hole corresponds to the top dead center of the flywheel, which is used to calibrate the ignition timing or injection timing, and adjust the valve clearance. When the relative position error between threaded holes and the reference plane of the crankshaft journal is too large, it will affect the dynamic balance of the crankshaft and flywheel, increase the friction and even scrap the crankshaft [1]–[3]. The error of the pin hole position will cause the ignition timing does not correspond to the piston stroke, resulting in insufficient fuel combustion, increased fuel consumption and exhaust exceeded. E Pipitone declined that the 1° angle error of the crankshaft can cause up to 10% evaluation error on IMEP (Indicated Mean Effective Pressure) and 25% error on the heat released by the combustion [4].

Therefore, for mass-produced crankshaft, it is very important to measure the relative position of the flange-end holes in industrial manufacturing. In the crankshaft-manufacturing workshop, the measurement of the relative position of flange-end holes is carried out in the semi-finished stage. By quantitatively measuring the relative position error of holes, the crankshaft can be corrected in the subsequent machining process.

As shown in Fig. 1, for the semi-finished crankshaft of the four-cylinder engine, the journal reference plane is composed of the centerline of the 1st, 5th main journal and the center of the 1st crank journal, and the flange-end is perpendicular to this journal reference plane. The distance error between the pin hole and the outer circle of the flange-end should not exceed 40 μm, and the position error of the threaded hole is not more than 0.1 mm.

The crankshaft full-parameter measuring instrument (or called crankshaft gauge) has extremely high precision, and crankshaft manufacturers use it to carry out selective inspection for the finished crankshaft. This instrument can measure the diameter, roundness, cylindricity, radial run-out, taper and

The associate editor coordinating the review of this manuscript and approving it for publication was Qilian Liang.

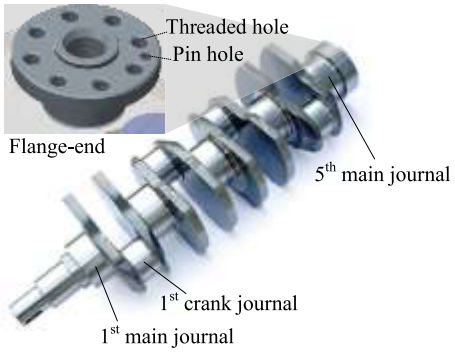

FIGURE 1. Flange-end holes and journals.

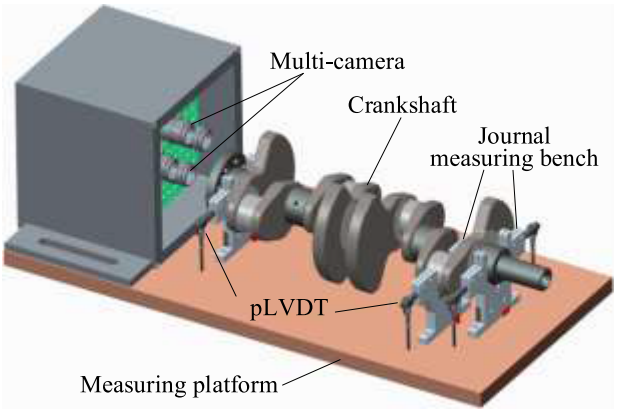

FIGURE 2. The diagram of the relative position measuring system of flange-end holes.

other information of the crank-shaft journal, and the measuring accuracy can reach 1 μm. However, the measurement results cannot provide the position of the flange-end holes, moreover, as a high precision measuring instrument, it can only measure the finished crankshaft with the smooth surface of the journal, and so it is not suitable for the semi-finished crankshaft with rough journal surface in machining process.

Common measuring methods for the flange-end holes position are: special Go/No go gauge, universal measuring microscope and CMM (coordinate measuring machine), etc. The special Go/No go gauge is a disc with the same size as the flange-end, on which a corresponding number of short pins are mounted to simulate the location of screws of the flywheel. This method is easy to operate and allows full inspection of the product in the manufacturing line. However, it can only judge the flange-end qualitatively, incapable of the deviation degree and direction of the position error. Universal measuring microscope uses the main microscope to measure the outline image of the work-piece, it has high fitting precision for the center of threaded holes, and measurement speed is fast, but the measured position information of the holes is not associated with the journal reference plane [5]. CMM uses contact probe to obtain points cloud of flange-end holes and journals, and the software fits the position information of the holes relative to the journal reference plane. CMM has the advantage of high accuracy, but it is only suitable for sampling inspection of mass production [6].

In order to achieve automatic measurement of the relative position of flange-end holes in the flexible manufacturing site, we propose a measurement system combines contact and visual measurement. The system contains pLVDT to measure the center position of the journal, which is an inductive displacement sensor with a shrink probe in non-measuring state. The probe protrudes to measure displacement with one bar air pressure, so that the inspection system can facilitate the automatic loading and unloading during the measuring process. A large-scale visual measurement device consisting of multi-camera to measure the coordinates of the flange-end holes, then the visual coordinate system convert into the global coordinate system of the journal reference plane, finally, the measurement system can calculate the position of flange-end holes relative to the journal reference plane. This method has the advantages of fast speed and high accuracy, and the measurement process can be implemented on-machine or in-situ, which facilitates the full detection of the mass-produced crankshaft in industrial manufacturing line.

II. THE PRINCIPLE OF THE RELATIVE POSITION MEASUREMENT

Flange-end holes relative position measuring system consist of two parts: the measurement of the reference plane that consists of journals, and the position measurement of threaded holes and pin hole on the flange-end.

The visual device obtains the chamfering profile of the flange-end holes for position measurement, and then it uses image detection processes to get the relative position of holes. The connection line between the center of the pin hole and the center of the flange-end contour is selected as the reference plane, so the visual device can determine whether the threaded hole is within the tolerance band of the manufacturing process. The relative position between the pin hole and the journal reference plane is recognized by measuring the deviation of the center of the pin hole from this plane, which puts forward the requirement for the measurement of the journal center. The system uses contact probes to measure the journal reference plane. There are 3 V-blocks on the crankshaft measuring platform to support the 1st, 5th spindle journals and the 1st crank journal respectively, and three pLVDTs are mounted on each V-block to form the measuring bench for measuring the cross-section center of the journal. Therefore, the system can get the position of the journal reference plane relative to the crankshaft measuring platform with the three journal measuring benches [7].

According to the requirements and the measurement principle of each part, the structure of the flange-end holes relative position measuring system is as follows:

A. THE SELECTIO AND MEASUREMENT OF THE JOURNAL REFERENCE PLANE

As the journal reference plane is defined by the center of the 1st, 5th spindle journals and the 1st crank journal, an ideal

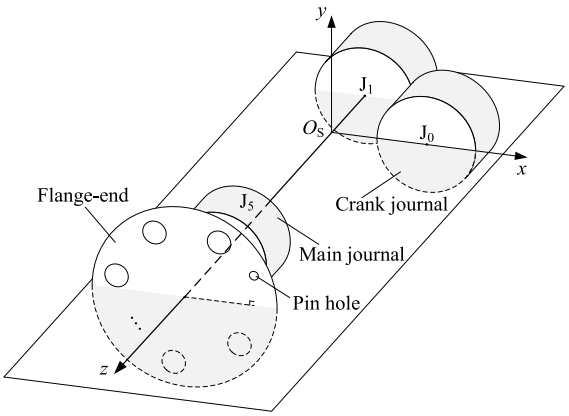

FIGURE 3. The global coordinate system O_s-xyz.

crankshaft can be placed in the measurement system, installed in place and to establish the global coordinate system O_s-xyz. As shown in Fig. 3, set the centerline J_1J_5 of the 1st, 5th main journals as the O_s-z axis, the O_s-x axis is the direction that passes through the center point J_0 of the 1st crank journal, and the intersection point of the O_s-x axis and the O_s-z axis is defined as the origin O_s, the upward direction perpendicular to the O_s-xy plane is set to the O_s-y axis.

For this ideal crankshaft, the reference plane of the flange-end holes is the O_s-xz plane. However, journal diameters of the semi-finished crankshafts being measured are not equal, resulting in a deviation of the actual journal reference plane from the ideal reference plane. The purpose of the journal measuring benches in the measuring system is to obtain the position of the actual journal reference plane in the global coordinate system O_s-xyz. Since the center of the journal is virtual, the system fits the center by measuring the outer contour of the journal [8]. The structure of the V-block and the distribution of pLVDTs is shown in Fig. 4a.

pLVDT, or called pneumatic push contact probe (PPCP), has a gaiter between probe tip and LVDT (Linear Variable Differential Transformer), as shown in Fig. 4b. Unlike the pneumatic gauge that senses displacement through changes in air pressure, pLVDT relies on pneumatic switching to control the expansion or contraction of the gaiter, pushing the LVDT's probe tip for contact measurement. It only contacts the measured surface at the moment of measurement, and this "pseudo non-contact" facilitates the automation of the measurement process. Since there is no air tightness requirement and accuracy as low as 0.1 μm, its low cost makes it widely used in industrial sites.

Two pLVDTs are mounted on both sides of the V-block, and the other one is mounted on the bottom. With the contact points of the three pLVDTs on the cross section of the journal, the system fits the diameter of the journal and its center coordinates relative to the V-block by the data of pLVDTs. Through the combined measurement of multiple measuring benches, we can calculate the relative position of the 1st, 5th main journals and the 1st crank journal. The tip of pLVDT is

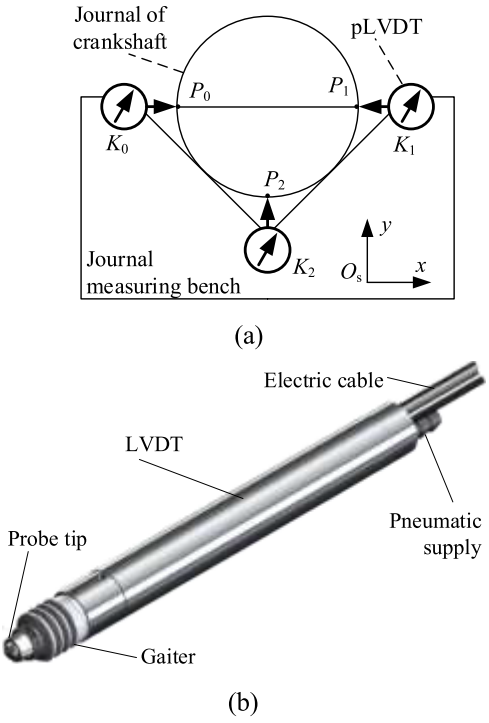

FIGURE 4. pLVDT and the journal measuring bench. (a) The diagram of journal measuring bench. (b) The composition of pLVDT.

a cylinder with 1 mm diameter, which provides line contact between pLVDT and journal surface of the semi-finished crankshaft. So pLVDT can eliminate the roundness error of the journal cylindrical surface effectively.

For the m-th journal to be measured, two horizontally opposed pLVDT (K_0, K_1) ensure that the distance of the two contact points P_0P_1 is equal to the diameter R_m of the journal, and the installation direction of pLVDT (K_2) at the bottom is perpendicular to P_0P_1. Before the measurement, a finished crankshaft with known diameter R_{m_std} for each journal can be used to calibrate these pLVDTs. The measurement system sets up the global coordinate system O_s-xyz by placing this finished crankshaft into the crankshaft measuring platform as the ideal crankshaft, and records the data k_{ref_n} of each pLVDT as its calibration value.

Set the measured data of pLVDT are k_n, the diameter R_m of the m-th journal can be obtained by:

$$R_m = R_{m\_std} - (k_0 - k_{ref\_0}) - (k_1 - k_{ref\_1}) \tag{1}$$

In the global coordinate system O_s-xyz, the center J_n of the m-th journal can be expressed as:

$$\begin{cases} x_m = \dfrac{(k_0 - k_{ref\_0}) - (k_1 - k_{ref\_1})}{2} \\ y_m = \left(\dfrac{R_m}{2} - \dfrac{R_{m\_std}}{2}\right) + (k_2 - k_{ref\_2}) \\ z_m = (m-1)\,L \end{cases} \tag{2}$$

In the above equation, L is the center distance between two adjacent main journals, and it is a fixed value. By calculating

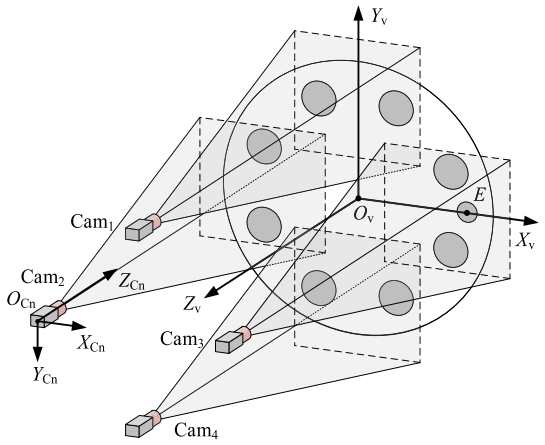

FIGURE 5. The structure of the flange-end visual measurement device.

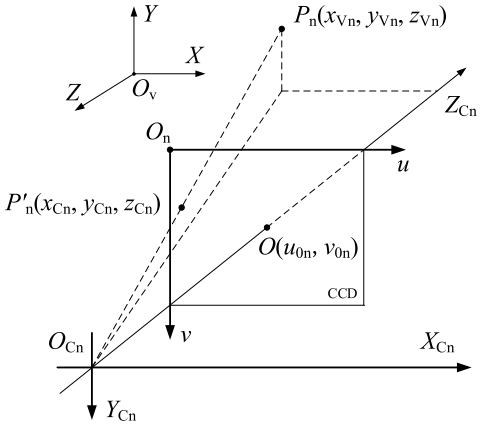

FIGURE 6. The pixel coordinate system O_n-uv and the sub-camera coordinate system O_{Cn}-xyz.

the central coordinates of the 1st, 5th main journals and the 1st crank journal, the system can get the plane equation of the journal reference plane in O_s-xyz.

B. THE MEASUREMENT OF THE FLANGE-END HOLES

The diameter of the flange-end of the crankshaft to be tested is $R_F = 80.5$ mm, and the positioning resolution of the hole is required to be 10 μm. Compare with the range of measurement, the accuracy of the visual system needs to be 0.125 %. If the system realizes the accuracy by a single camera, high-resolution camera and sub-pixel imaging processing technology are needed, all of which have high requirements for the illumination, pixel size and imaging effect of the camera. Due to the implementation cost and technical difficulty of the single camera vision measurement, the system chooses the multi-camera fusion measurement method to achieve high-procession measurement for this large-size object [9]–[11].

The large-scale visual measurement device is made up of four industrial cameras in the experiment. For installing cameras, in order to extract all the outlines of the flanges, there is no need for the overlapping areas in the camera field of view, which can improve the measuring range and meet the high measurement precision requirements under the large field of view [12], [13]. The final multi-camera structure is as follows:

Before the measurement of the vision system for the flange-end holes, it is necessary to calibrate each sub-camera in the visual measurement device. The calibration processes are: 1. the calibration of the intrinsic parameters of sub-camera; 2. global calibration for fusion progress of each pixel coordinate system to the flange-end surface coordinate system (this is also the process for calculating the extrinsic parameters of each sub-camera) [14].

For the n-th sub-camera, a 2D pixel coordinate system O_n-uv is set up with the upper left corner of the CCD as its origin O_n, sets the horizontal direction of the CCD as the O_n-u axis, and the vertical downward direction is the O_n-v axis, as shown in Fig. 6. Meanwhile, take the perspective projection center as the origin O_{Cn}, a corresponding 3D sub-camera coordinate system O_{Cn}-xyz is established, takes the direction of optical axis of the sub-camera as the O_{Cn}-z axis, its O_{Cn}-z axis and O_{Cn}-z axis are parallel to the O_n-u axis and the O_n-v axis, respectively.

For the transformation formula between the imaging point (u_n, v_n) in the pixel coordinate system O_n-uv and $P'_n(x_{Cn}, y_{Cn}, z_{Cn})$ in O_{Cn}-xyz, it can be expressed as:

$$z_{Cn}\begin{bmatrix} u_n \\ v_n \\ 1 \end{bmatrix} = \begin{bmatrix} f_n/dx_n & 0 & u_{0n} & 0 \\ 0 & f_n/dy_n & v_{0n} & 0 \\ 0 & 0 & 1 & 0 \end{bmatrix}\begin{bmatrix} x_{Cn} \\ y_{Cn} \\ z_{Cn} \\ 1 \end{bmatrix} \quad (3)$$

For the n-th sub-camera, (u_{0n}, v_{0n}) is the intersection point of the optical axis (O_{Cn}-z axis) and the O_n-uv plane, and f_n is the effective focal length of this sub-camera. dx_n and dy_n refer to the physical dimensions of each pixel of the CCD, usually expressed by $f_{xn} = f_n/dx_n$ and $f_{yn} = f_n/dy_n$. Finally, f_{xn}, f_{yn}, u_{0n} and v_{0n} are the sub-camera intrinsic parameters to be calibrated.

By calculating the conversion formula between the pixel coordinate system and the flange-end surface coordinate system, we can get the extrinsic parameters of the sub-camera relative to the flange-end surface [15]. The flange-end surface coordinate system O_v-xyz is set up by taking the center of the flange-end contour as the origin O_v. E is the center point of the pin hole, and the O_v-x axis is established based on the centerline O_vE between the pin hole and the flange-end contour. The O_v-y axis is perpendicular to the O_v-x axis on the flange-end surface, and the O_v-z axis is a vertical line through the center of the flange-end, as shown in Fig. 6.

In the process of using checkerboard to calibrate the sub-camera, without the relative position of the common feature points such as the pin hole, we cannot directly calculate the conversion relation between O_{Cn}-xyz and O_v-xyz. Fine-tuning the checkerboard so that it coincides with the actual flange-end surface, and use this checkerboard plane to establish a transitional coordinate system O_B-xyz. $\boldsymbol{R}_{Cn}\boldsymbol{T}_{Cn}$ is set as the translation matrix between O_{Cn}-xyz and O_B-xyz, for the point

$P'_{\mathrm{n}}(x_{\mathrm{Cn}}, y_{\mathrm{Cn}}, z_{\mathrm{Cn}})$ in O_{Cn}-xyz, its conversion relationship is expressed as follows:

$$\begin{bmatrix} x_{Cn} \\ y_{Cn} \\ z_{Cn} \\ 1 \end{bmatrix} = \begin{bmatrix} R_{Cn} & T_{Cn} \\ 0^T & 1 \end{bmatrix} \begin{bmatrix} x_B \\ y_B \\ z_B \\ 1 \end{bmatrix} \tag{4}$$

As the O_{B}-xy plane coincides with the O_{v}-xy plane, for the transformation matrix $\boldsymbol{R}_{\mathrm{BV}}\boldsymbol{T}_{\mathrm{BV}}$ between O_{B}-xyz and O_{v}-xyz, there are only translation and rotation in the two-dimensional plane. The characteristic point $(x_{\mathrm{B}}, y_{\mathrm{B}}, z_{\mathrm{B}})$ in the transitional coordinate system can be expressed as follows:

$$\begin{bmatrix} x_B \\ y_B \\ z_B \\ 1 \end{bmatrix} = \begin{bmatrix} R_{BV} & T_{BV} \\ 0^T & 1 \end{bmatrix} \begin{bmatrix} x_{Vn} \\ y_{Vn} \\ z_{Vn} \\ 1 \end{bmatrix} \tag{5}$$

For the n-th sub-camera, with Eqs (3), (4) and (5), the conversion relationship between O_{n}-uv and O_{v}-xyz can be expressed as follows:

$$z_{Cn} \begin{bmatrix} u_n \\ v_n \\ 1 \end{bmatrix} = \begin{bmatrix} f_{xn} & 0 & u_{0n} & 0 \\ 0 & f_{xn} & v_{0n} & 0 \\ 0 & 0 & 1 & 0 \end{bmatrix} \begin{bmatrix} R_{Cn} & T_{Cn} \\ 0^T & 1 \end{bmatrix} \times \begin{bmatrix} R_{BV} & T_{BV} \\ 0^T & 1 \end{bmatrix} \begin{bmatrix} x_{Vn} \\ y_{Vn} \\ z_{Vn} \\ 1 \end{bmatrix} \tag{6}$$

In the above formula, both $\boldsymbol{R}_{\mathrm{Cn}}\boldsymbol{T}_{\mathrm{Cn}}$ and $\boldsymbol{R}_{\mathrm{BV}}\boldsymbol{T}_{\mathrm{BV}}$ are extrinsic parameters of the n-th sub-camera relative to the flange-end.

For the calibration of the intrinsic parameters (f_{xn}, f_{yn}, u_{0n} and v_{0n}) and extrinsic ($\boldsymbol{R}_{\mathrm{Cn}}\boldsymbol{T}_{\mathrm{Cn}}$ and $\boldsymbol{R}_{\mathrm{BV}}\boldsymbol{T}_{\mathrm{BV}}$) parameters of the flange-end visual measurement device, due to its large field of view and high calibration accuracy, Zhang's method is used to calibrate the intrinsic and extrinsic parameters of sub-cameras [16], [17].

For the calibration of the intrinsic parameter of the sub-camera in the experiment, the position of the flange-end visual measurement device is fixed. The checkerboard is randomly placed 16 times, so that each sub-camera can get 16 checkerboard images respectively. In the global calibration process, the checkerboard is kept coincident with the actual flange-end face, and each sub-camera then obtains a static checkerboard image.

In the process of calculating the intrinsic parameters for each sub-camera [18], the single static checkerboard image obtained from the global calibration process is taken as the first image, and the 16 images captured during the intrinsic parameter calibration process are arranged in the subsequent sequence, and a total of 17 checkerboard images are involved in the calculation of the intrinsic parameters. By the corresponding relation between the checkerboard corners and the imaging feature points of sub-camera, the intrinsic parameters (f_{xn}, f_{yn}, u_{0n} and v_{0n}) and 17 $\boldsymbol{RT}$ matrices can be calculated.

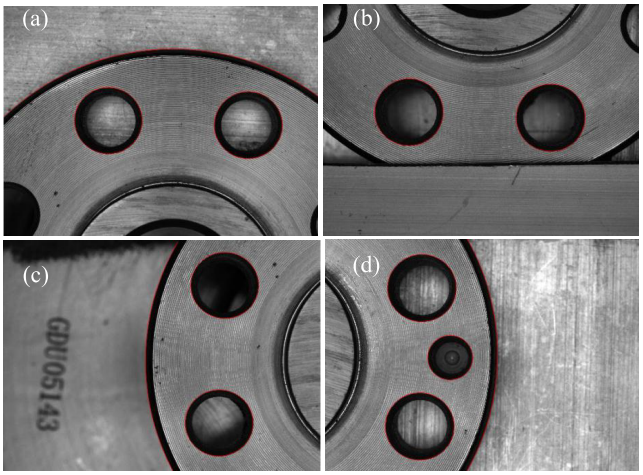

FIGURE 7. Four sub-camera hole edge detection results. (a) Cam1 edge detection. (b) Cam4 edge detection. (c) Cam2 edge detection. (d) Cam3 edge detection.

For the $\boldsymbol{RT}$ matrix calculated by the first checkerboard image in the global calibration process, it is also the conversion matrix $\boldsymbol{R}_{\mathrm{Cn}}\boldsymbol{T}_{\mathrm{Cn}}$ between O_{Cn}-xyz and O_{B}-xyz. Meanwhile, using the pin hole and the center of the flange-end contour as common points, the conversion matrix $\boldsymbol{R}_{\mathrm{BV}}\boldsymbol{T}_{\mathrm{BV}}$ between the transitional coordinate system O_{B}-xyz and the flange-end surface coordinate system O_{v}-xyz can be obtained.

After calibrating the visual measurement device, we can get partial images of the flange-end holes through these four sub-cameras. By locating the detection area of these partial images, the contour area of the flange end can be obtained, such as threaded holes, pin hole and the outer circle. For the contour areas, the Canny operator is used for edge detection to obtain pixel-level contours, and sub-pixel level contours are obtained based on bilinear interpolation [19], [20]. Finally, contours are shown in Fig. 7.

After each sub-camera performs a distortion correction on the contours, all the contour points in the pixel coordinate system O_{n}-uv are converted to the flange-end surface coordinate system O_{v}-xyz by Eq. (6). After the contours are stitched, by using the least square method to fit threaded holes, pin hole and the outer circle center [21], the final positional relationship between the pin hole and threaded holes in the flange-end surface coordinate system is shown in Fig. 8.

III. THE UNIFICATION OF THE FLANGE-END VISUAL MEASUREMENT DEVICE AND JOURNAL REFERENCE PLANE

The hole coordinate measured by the flange-end visual measurement device is meaningful only in the O_{v}-xy plane, and is a fixed value in the depth direction O_{v}-z. The global coordinate system O_{s}-xyz in the flange-end holes measurement is 3D, so when measuring the position of the pin hole relative to the journal reference plane, the 2D coordinate values of the flange-end holes need to be converted into the global coordinate system O_{s}-xyz [22]. In the coordinate system

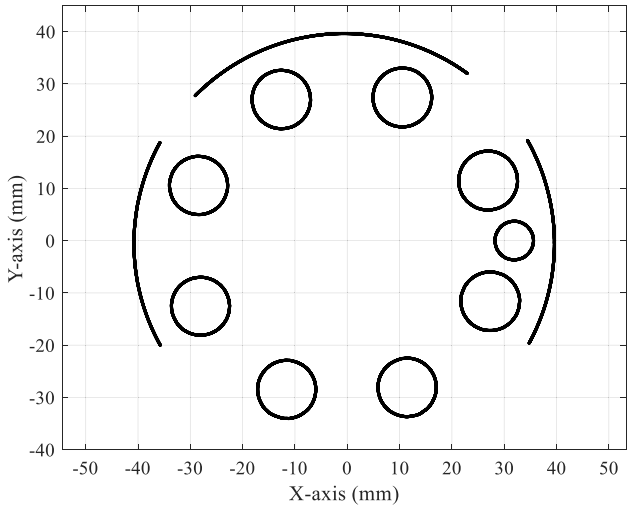

FIGURE 8. The contour splicing of the flange-end holes.

transformation between O_s-xyz and O_v-xyz, the seven-parameter transformation model (Bursa-Wolf model) is expressed as follows:

$$\begin{bmatrix} x_S \\ y_S \\ z_S \end{bmatrix} = \lambda R_{V2S} \begin{bmatrix} x_V \\ y_V \\ z_V \end{bmatrix} + T_{V2S} \tag{7}$$

$\boldsymbol{R}_{\mathrm{V2S}}$ is the rotation matrix of O_v-xyz to O_s-xyz, set ε_x, ε_y, and ε_z as rotation angles around the X-, Y- and Z-axis in O_s-xyz, and $\boldsymbol{T}_{\mathrm{V2S}} = [\Delta x, \Delta y, \Delta z]^{\mathrm{T}}$ is the transfer matrix [23]. For the semi-finished crankshaft after rough machining, it can be regarded as a rigid body without considering thermal expansion, there is no scale deformation in the measurement process, so, the scale factor $\lambda = 0$. As the flange-end surface is perpendicular to the journal reference plane, the rotation angles $\varepsilon_x = \varepsilon_y = 0$, so the Eq. (7) can be simplified as:

$$\begin{bmatrix} x_S \\ y_S \\ z_S \end{bmatrix} = \begin{bmatrix} \cos\varepsilon_z & \sin\varepsilon_z & 0 \\ -\sin\varepsilon_z & \cos\varepsilon_z & 0 \\ 0 & 0 & 0 \end{bmatrix} \begin{bmatrix} x_V \\ y_V \\ z_V \end{bmatrix} + \begin{bmatrix} \Delta x \\ \Delta y \\ \Delta z \end{bmatrix} \tag{8}$$

In the experiment, a finished crankshaft is used to calculate the conversion matrix $\boldsymbol{RT}_{\mathrm{V2S}}$, which has a good roundness and roughness of journals and flange-end surface. By using the Adcole crankshaft gauge, the mutual position and diameter R_{m_std} of each journal can be obtained.

Then, the relative positions of the flange-end holes are measured by a CMM (PMM-XI of Leitz Ltd.), and their position relative to the journal reference plane. The CMM measuring coordinate system is based on the plane formed by the 1st, 5th main journals, and the 1st crank journal. In the process of fitting the central coordinate of the journal by using the point clouds of the CMM, the diameter R_{m_std} measured by the Adcole crankshaft gauge is substituted to improve the fitting accuracy, and the calibration difficulty of the measurement system is reduced. Finally, the CMM can directly measure the coordinates of journals and flange-end holes in the global coordinate system O_s-xyz.

In unification between O_s-xyz and O_v-xyz, using this finished crankshaft with known position information as the ideal crankshaft that mentioned in Section 2.A, and the initial measuring value of the pLVDT on the V-block is the calibrated value $k_{\mathrm{ref\_n}}$ in Eq. (2). The flange-end hole coordinate (x_S, y_S, z_S) in O_s-xyz can be obtained directly, because the CMM measuring coordinate system is equivalent to the global coordinate system O_s-xyz, and coordinate (x_V, y_V, z_V) in O_v-xyz can be measured by the visual measurement device. By the coordinates of the flange-end holes in two different coordinate systems, the conversion matrix $\boldsymbol{RT}_{\mathrm{V2S}}$ can be calibrated by the Eq. (8).

IV. THE UNCERTAINTY ANALYSIS OF THE RELATIVE POSITION MEASUREMENT

Due to the roundness and roughness error of journals of the semi-finished crankshaft, there is an error in the central coordinate measurement by the journal measuring bench. For the semi-finished crankshaft after rough machining, the roundness error of journal is $\Delta_{\mathrm{round}} = 50\ \mu$m, so the central coordinate error Δ_{axis} introduced by three pLVDTs can be expressed as:

$$\begin{aligned}
&x_m(k_0, k_1) \\
&= \frac{(k_0 - k_{ref_0}) - (k_1 - k_{ref_1})}{2} \\
&y_m(k_0, k_1, k_2) \\
&= (k_2 - k_{ref_2}) - \left(\frac{(k_0 - k_{ref_0}) + (k_1 - k_{ref_1})}{2}\right) \\
&\Delta k_0 \\
&= \Delta k_1 = \Delta k_2 = \sqrt{\Delta^2_{round} + \Delta^2_{sen}} \\
&\Delta x_m \\
&= \sqrt{\left(\frac{\partial x_m}{\partial k_0}\right)^2 (\Delta k_0)^2 + \left(\frac{\partial x_m}{\partial k_1}\right)^2 (\Delta k_1)^2} \\
&= \sqrt{\frac{1}{4}(\Delta k_0)^2 + \frac{1}{4}(\Delta k_1)^2} \\
&\Delta y_m \\
&= \sqrt{\left(\frac{\partial x_m}{\partial k_0}\right)^2 (\Delta k_0)^2 + \left(\frac{\partial x_m}{\partial k_1}\right)^2 (\Delta k_1)^2 + \left(\frac{\partial x_m}{\partial k_2}\right)^2 (\Delta k_2)^2} \\
&= \sqrt{\frac{1}{4}(\Delta k_0)^2 + \frac{1}{4}(\Delta k_1)^2 + (\Delta k_2)^2} \\
&\Delta_{axis} \\
&= \sqrt{\Delta x_m^2 + \Delta y_m^2}
\end{aligned} \tag{9}$$

In the experiment, the DP/5/P model pLVDT from Solartron Metrology Ltd, UK is used, its full-scale range is 5 mm and the linearity is 0.05%. The measurement uncertainty of single pLVDT is $\Delta_{\mathrm{sen}} = 2.5\ \mu$m, and the measurement error Δk_{n} is represented by Δ_{round} and Δ_{sen}, so the central coordinate error $\Delta_{\mathrm{axis}} = 71.37\ \mu$m.

For the actual journal reference plane S' formed by the semi-finished crankshaft to be measured, and the ideal plane S formed by the finished crankshaft. There is an inclination

angle between S' and S due to the unequal journal diameters and roundness errors. Therefore, in the conversion of the flange-end surface coordinate system O_V-xyz and the global coordinate system O_s-xyz, and it is necessary to compensate this inclination angle to Eq. (7).

Set the conversion matrix between S' and S plane is $\boldsymbol{RT}_{\text{meas}}$, and the rotation matrix $\boldsymbol{R}_{\text{meas}}$ consists of yaw angle ψ, pitch angle θ, and roll angle φ [24]. For the semi-finished crankshaft to be measured, while the diameters of the 1st and 5th main journal are not equal, there is the pitch angle θ between S' and S plane, and the yaw angle ψ between S' and S plane is due to the roundness error of journals. For the semi-finished crankshaft and ideal crankshaft, the roll angle φ formed by the plane S' around the O_s-z axis is due to the different diameters of the 1st crank journal, meanwhile, as the unequal diameters of journals, there is an transfer matrix $\boldsymbol{T}_{\text{meas}}$ between the actual journal reference plane S' and the ideal journal reference plane S.

For the central coordinate $[x'_S, y'_S, z'_S]$ measured by the journal measuring bench in the global coordinate system O_s-xyz, the conversion relationship with the coordinate $[x_S, y_S, z_S]$ on the ideal journal reference plane is as follows:

$$\begin{bmatrix} x'_S \\ y'_S \\ z'_S \end{bmatrix} = R_{meas} \begin{bmatrix} x_S \\ y_S \\ z_S \end{bmatrix} + T_{meas} \tag{10}$$

For the diameter error between the 1st and 5th main journal, the pitch angle θ can be expressed as:

$$\theta = \arctan\left(\frac{\Delta_R}{2L}\right) \tag{11}$$

For different main journals, the diameter error Δ_R caused by rough machining is 0.1 mm, and the center distance of journals in the O_s-z direction is $L = 86$ mm, so the pitch angle $\theta = 0.033°$.

The yaw angle ψ is mainly composed of the installation error $\Delta_{V-block}$ of the V-block and the center error Δ_{axis} of journals, so ψ is expressed as:

$$\psi = \arctan\left(\frac{\sqrt{\Delta^2_{V-block} + \Delta^2_{axis}}}{2L}\right) \tag{12}$$

The installation error of the V-block is depended on the machining baseline of the measuring platform, which is machined by the linear cutting of CNC machine tools. Machining accuracy of a general CNC can be guaranteed to be better than 10 μm, so the installation error of V-block is $\Delta_{V-block} = 0.01$ mm, and the yaw angle error $\psi = 0.017°$.

As the flange-end is rigidly connected to the 1st main journal, the variation of the journal reference plane can also cause errors at the flange-end visual measurement device. This is mainly due to the fact that the flange-end surface is not perpendicular to the optical axis of the visual measurement device, and this vertical angle β is composed of the pitch angle θ and the yaw angle ψ of the semi-finished crankshaft.

$$\beta = \arctan\sqrt{(\tan\theta)^2 + (\tan\psi)^2} \tag{13}$$

For the measurement error caused by the vertical angle β between the flange-end surface and the optical axis, the maximum distance of the flange-end surface: the diameter error Δ_F of the outer circle is set as an example to illustrate:

$$\Delta_F = R_F(1-\cos\beta) = R_F\left(1-\sqrt{\frac{1}{1+(\tan\theta)^2+(\tan\psi)^2}}\right) \tag{14}$$

The maximum distance measurement error caused by θ and ψ is $\Delta_F = 0.017$ μm, so the measurement error of the flange-end surface caused by the vertical angle β can be ignored. Therefore, set $\psi = \theta = 0$, and Eq. (10) can be simplified as follows:

$$\begin{bmatrix} x'_S \\ y'_S \\ z'_S \end{bmatrix} = \begin{bmatrix} \cos\varphi & \sin\varphi & 0 \\ \sin\varphi & \cos\varphi & 0 \\ 0 & 0 & 0 \end{bmatrix} \begin{bmatrix} x_S \\ y_S \\ z_S \end{bmatrix} + T_{meas} \tag{15}$$

By the central coordinate $[x'_S, y'_S, z'_S]$ of journals obtained by the measuring bench, and the known ideal journal reference plane, the roll angle φ and transfer matrix $\boldsymbol{T}_{\text{meas}}$ can be calculated by Eq. (15).

In O_s-xyz, by substituting Eq. (8) into Eq. (15), the coordinates of the flange-end holes are compensated by the following equation:

$$\begin{bmatrix} x'_S \\ y'_S \\ z'_S \end{bmatrix} = \begin{bmatrix} \cos\varphi & \sin\varphi & 0 \\ -\sin\varphi & \cos\varphi & 0 \\ 0 & 0 & 0 \end{bmatrix} \times \begin{bmatrix} x_v\cos\varepsilon z + y_v\sin\varepsilon z + \Delta x \\ -x_v\sin\varepsilon z + y_v\cos\varepsilon z + \Delta y \\ \Delta z \end{bmatrix} + T_{meas} \tag{16}$$

For the uncertainty Δ_V of the flange-end visual measurement device in the measuring of the semi-finished crankshaft, the actual flange-end surface is not exactly coincident with the plane of the checkerboard while calibrating sub-camera. And the illumination, the chamfer of threaded holes, and the reflected light from the flange-end surface, etc., all of which will affect the uncertainty of the flange-end holes relative position measurement [25].

The uncertainty Δ_V of the flange-end visual measurement device is verified by a custom-made flange-end model, which has correspondingly machined threaded holes and pin hole. ZIP250 multisensor (OGP SmartScope Ltd, Singapore) measures the mutual position between threaded holes and pin hole as the true value, as shown in Fig. 9.

Then thread holes on the custom-made flange-end model are chamfered and tapped, in order to simulate the actual flange-end surface of the semi-finished crankshaft. The processed flange-end model is measured by the visual measurement device, and the values are compared with the true values from the ZIP250 multisensor. Set the pin hole and the outer circle as the grid-reference, and the coordinate error of each threaded hole is shown in Fig. 10. The final uncertainty $\Delta_V = 0.04$ mm.

In the flange-end holes relative position measuring system, the final measurement uncertainty Δ_{Err} is influenced by: the

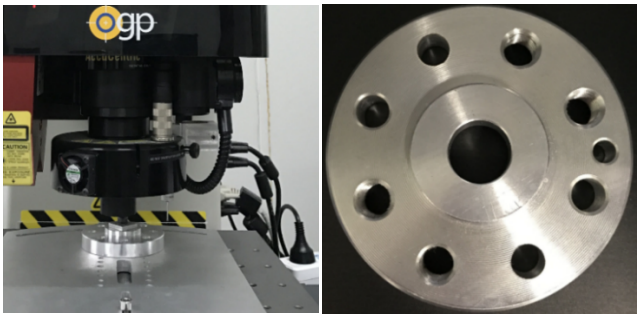

FIGURE 9. The calibration of the custom-made flange-end. (a) Measuring the flange-end model with multisensor. (b) Custom-made flange-end model and its holes.

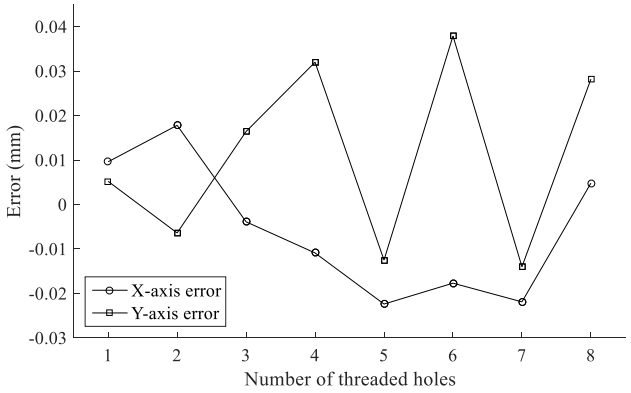

FIGURE 10. The uncertainty of the visual measurement device.

uncertainty Δ_V of the visual measurement device, the central coordinate uncertainty Δ_{axis} of journals, and the inclination error of the journal reference plane [26]. By calculating the conversion matrix $\boldsymbol{RT}_{meas}$, and compensated it to the visual measurement result, to eliminate the inclination error of the reference plane. Flange-end holes relative position measurement uncertainty Δ_{Err} is approximately calculated by:

$$\Delta_{Err} = \sqrt{\Delta_V^2 + \Delta_{axis}^2} \tag{17}$$

From the Eq. (17), the measurement uncertainty of the flange-end holes of semi-finished crankshaft is $\Delta_{Err} = 81.8\ \mu$m.

V. EXPERIMENT AND ANALYSIS

To verify the measuring system for the flange-end holes relative position, a semi-finished crankshaft is scanned by CMM to get the relative position of flange-end holes as the true value, the flange-end holes relative position measuring system is finally showed in Fig. 11.

By collecting the central coordinates of journals and the flange-end holes coordinates from the visual measurement device, so the compensated coordinates of the flange-end holes relative to the journal reference plane can be calculated by Eq. (16), and the single measurement takes less than 30 seconds. For the relative position of the pin hole

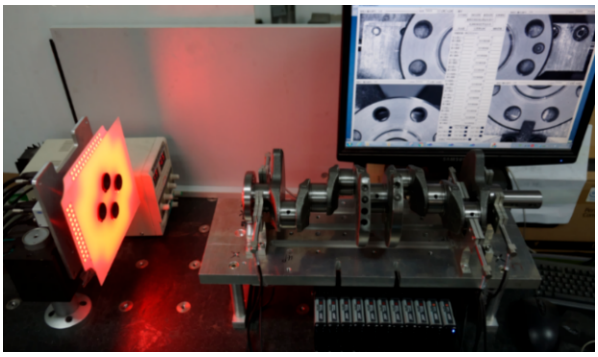

FIGURE 11. The object of the flange-end holes relative position measuring system.

TABLE 1. The measurement error of the flange-end holes.

No.	x(mm)	y(mm)	No.	x(mm)	y(mm)
Pin hole	-0.005	0.006	Outer circle	-0.003	0.009
Threaded hole 1	0.024	0.052	Threaded hole 5	-0.097	-0.09
Threaded hole 2	-0.022	-0.025	Threaded hole 6	-0.084	0.042
Threaded hole 3	-0.042	-0.036	Threaded hole 7	-0.058	-0.023
Threaded hole 4	-0.058	-0.016	Threaded hole 8	-0.048	-0.014

and threaded holes, the difference between the measurement result and CMM true value is given in table 1:

As shown in Table 1, the standard deviation of the relative position of the flange-end holes is 0.041 mm, and the maximum deviation of the threaded hole is 0.097 mm, which can meet the 0.01 mm measurement error requirement of flange-end holes in semi-finished crankshaft machining line.

VI. CONCLUSION

For the position measurement of the flange-end holes of semi-finished crankshaft relative to the journal reference plane, this paper presents a rapid flange-end holes relative position measuring system. Journal measuring benches made of pLVDT are used to get the position of the journal reference plane, and central coordinates of the flange-end holes are obtained by the multi-camera measurement device. Through coordinate system transformation, the coordinate of the flange-end holes is integrated into the global coordinate system composed of the journal reference plane, and finally get the relative position between the flange-end holes and the journal reference plane. In the experiment, a finished crankshaft with good roundness and roughness is used to calibrate the measurement system, and the measurement uncertainty of the flange-end holes relative position can be better than 0.1 mm. This relative position measurement system has the advantages of fast measurement speed and wide-range, and can greatly improve the detection efficiency of the crankshaft grinding workshop.

REFERENCES

[1] L. Witek, M. Sikora, F. Stachowicz, and T. Trzepiecinski, "Stress and failure analysis of the crankshaft of diesel engine," *Eng. Fail Anal.*, vol. 82, pp. 703–712, Dec. 2017.
[2] M. Fonte, P. Duarte, L. Reis, M. Freitas, and V. Infante, "Failure mode analysis of two crankshafts of a single cylinder diesel engine," *Eng. Fail Anal.*, vol. 56, pp. 185–193, Oct. 2015.
[3] I. Bickley, V. D'Olier, H. Fessler, T. H. Hyde, and N. A. Warrior, "Stresses and deformations in overlapped diesel engine crankshafts, Part 1: Experimental results," *Proc. Inst. Mech. Eng. D, J. Automobile Eng.*, vol. 212, no. 3, pp. 187–204, 1998.
[4] E. Pipitone and A. Beccari, "Determination of TDC in internal combustion engines by a newly developed thermodynamic approach," *Appl. Thermal Eng.*, vol. 30, nos. 14–15, pp. 1914–1926, 2010.
[5] F. J. Brosed, J. Santolaria, J. J. Aguilar, and D. Guillomía, "Laser triangulation sensor and six axes anthropomorphic robot manipulator modelling for the measurement of complex geometry products," *Robot Comput. Integr. Manuf.*, vol. 28, no. 6, pp. 660–671, 2012.
[6] A. B. Abdullah, S. M. Sapuan, and Z. Samad, "Roundness error evaluation of cold embossed hole based on profile measurement technique," *Int. J. Adv. Manuf. Technol.*, vol. 80, nos. 1–4, pp. 293–300, 2015.
[7] G. Wei and Q. Tan, "Measurement of shaft diameters by machine vision," *Appl. Opt.*, vol. 50, no. 19, pp. 3246–3253, 2011.
[8] M. Zhang and Z. Yao, "Grinding performance in crankshaft pin journal path-controlled grinding of 40Cr using CBN wheel," *Int. J. Adv. Manuf. Technol.*, vol. 82, nos. 9–12, pp. 1581–1586, 2016.
[9] C. Häne *et al.*, "3D visual perception for self-driving cars using a multi-camera system: Calibration, mapping, localization, and obstacle detection," *Image Vis. Comput.*, vol. 68, pp. 14–27, Dec. 2017.
[10] N. Zeller, F. Quint, and U. Stilla, "Depth estimation and camera calibration of a focused plenoptic camera for visual odometry," *ISPRS-J. Photogramm. Remote Sens.*, vol. 118, pp. 83–100, Aug. 2016.
[11] H. Bamberger, E. Hong, R. Katz, J. S. Agapiou, and S. M. Smyth, "Non-contact, in-line inspection of surface finish of crankshaft journals," *Int. J. Adv. Manuf. Technol.*, vol. 60, nos. 9–12, pp. 1039–1047, 2012.
[12] L. Yu, K. Wang, and G. Fan, "Photometric calibration and image stitching for a large field of view multi-camera system," *Sensors.*, vol. 16, no. 4, p. 516, 2016.
[13] D. Nilosek, D. J. Walvoord, and C. Salvaggio, "Assessing geoaccuracy of structure from motion point clouds from long-range image collections," *Opt. Eng.*, vol. 53, no. 11, 2014, Art. no. 113112.
[14] B. Sun, J. Zhu, L. Yang, S. Yang, and Z. Niu, "Calibration of line-scan cameras for precision measurement," *Appl. Opt.*, vol. 55, no. 25, pp. 6836–6843, 2016.
[15] A. Schmidt, A. Kasiński, M. Kraft, M. Fularz, and Z. Domagała, "Calibration of the multi-camera registration system for visual navigation benchmarking," *Int. J. Adv. Robot Syst.*, vol. 11, no. 6, p. 83, 2014.
[16] Z. Zhang, "A flexible new technique for camera calibration," *IEEE Trans. Pattern Anal. Mach. Intell.*, vol. 22, no. 11, pp. 1330–1334, Nov. 2000.
[17] F. Lahajnar, R. Bernard, F. Pernuš, and S. Kovačič, "Machine vision system for inspecting electric plates," *Comput. Ind.*, vol. 47, no. 1, pp. 113–122, 2002.
[18] M. Brückner, F. Bajramovic, and J. Denzler, "Intrinsic and extrinsic active self-calibration of multi-camera systems," *Mach. Vis. Appl.*, vol. 25, no. 2, pp. 389–403, 2014.
[19] Y. Bai and H. Zhuang, "On the comparison of bilinear, cubic spline, and fuzzy interpolation techniques for robotic position measurements," *IEEE Trans. Instrum. Meas.*, vol. 54, no. 6, pp. 2281–2288, Dec. 2005.
[20] P. Chainais, E. Kænig, V. Delouille, and J.-F. Hochedez, "Virtual super resolution of scale invariant textured images using multifractal stochastic processes," *J. Math. Imag. Vis.*, vol. 39, no. 1, pp. 28–44, 2011.
[21] Z. Gong, J. Sun, and G. Zhang, "Dynamic structured-light measurement for wheel diameter based on the cycloid constraint," *Appl. Opt.*, vol. 55, no. 1, pp. 198–207, 2016.
[22] C. Yu and Q. Peng, "A unified-calibration method in FTP-based 3D data acquisition for reverse engineering," *Opt. Lasers Eng.*, vol. 45, no. 3, pp. 396–404, 2007.
[23] T. Moons, L. Van Gool, M. Proesmans, and E. Pauwels, "Affine reconstruction from perspective image pairs with a relative object-camera translation in between," *IEEE Trans. Pattern Anal. Mach. Intell.*, vol. 18, no. 1, pp. 77–83, Jan. 1996.
[24] J. Jin, L. Zhao, and S. Xu, "High-precision rotation angle measurement method based on monocular vision," *J. Opt. Soc. Amer. A, Opt. Image Sci.*, vol. 31, no. 7, pp. 1401–1407, 2014.
[25] L. M. Xu, Z. Q. Yang, Z. H. Jiang, and Y. Chen, "Light source optimization for automatic visual inspection of piston surface defects," *Int. J. Adv. Manuf. Technol.*, vol. 91, nos. 5–8, pp. 2245–2256, 2017.
[26] D. Samper, J. Santolaria, F. J. Brosed, A. C. Majarena, and J. J. Aguilar, "Analysis of TSAI calibration method using two- and three-dimensional calibration objects," *Mach. Vis. Appl.*, vol. 24, no. 1, pp. 117–131, 2013.

LEI WANG is currently a Lecturer with the College of Electronic and Communication Engineering, Tianjin Normal University, China. His main research interests include measurement and sensor technology, electronics, and embedded systems.

GANG LU received the B.S. degree from Tianjin University, where he is currently pursuing the M.S. degree in instrument science and technology. His research interests include geometric measurement and sensor technology.

YING SUN received the B.S. degree from Tianjin University, where she is currently pursuing the M.S. degree in instrument science and technology. Her research interests include visual measurement and inertial technology.